

AD-A040 703

AIR FORCE GEOPHYSICS LAB HANSCOM AFB MASS  
METEOROLOGICAL SATELLITE MEASUREMENTS AND APPLICATIONS.(U)  
FEB 77 J T BUNTING, F R VALOVICIN, T J KEEGAN  
AFGL-TR-77-0035

F/G 22/2

UNCLASSIFIED

NL

1 OF 1

AD  
A040703



END

DATE  
FILMED  
7-77

AD A 040703

AFGL-TR-77-0035  
AIR FORCE SURVEYS IN GEOPHYSICS, NO. 362



## Meteorological Satellite Measurements and Applications

JAMES T. BUNTING  
FRANCIS R. VALOVICIN  
THOMAS J. KEEGAN

3 February 1977



Approved for public release; distribution unlimited.

METEOROLOGY DIVISION PROJECT 8628

**AIR FORCE GEOPHYSICS LABORATORY**

HANSCOM AFB, MASSACHUSETTS 01731

**AIR FORCE SYSTEMS COMMAND, USAF**

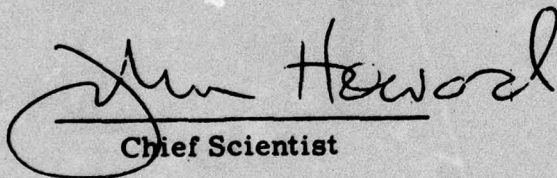


AD No. \_\_\_\_\_  
DDC FILE COPY

This report has been reviewed by the ESD Information Office (OI) and is releasable to the National Technical Information Service (NTIS).

This technical report has been reviewed and is approved for publication.

FOR THE COMMANDER

  
Chief Scientist

Qualified requestors may obtain additional copies from the Defense Documentation Center. All others should apply to the National Technical Information Service.

Unclassified

SECURITY CLASSIFICATION OF THIS PAGE (When Data Entered)

REPORT DOCUMENTATION PAGE		READ INSTRUCTIONS BEFORE COMPLETING FORM	
1. REPORT NUMBER	2. REPORT ACCESSION NO.	3. RECIPIENT'S CATALOG NUMBER	
14	AFGL-TR-77-0035, AFGL-AFSG-362		
4. TITLE (and Subtitle)	5. TYPE OF REPORT & PERIOD COVERED		
6	METEOROLOGICAL SATELLITE MEASUREMENTS AND APPLICATIONS.		
7. AUTHOR(s)	6. PERFORMING ORG. REPORT NUMBER		
10	AFSG No. 362, ✓		
	6. CONTRACT OR GRANT NUMBER(s)		
9. PERFORMING ORGANIZATION NAME AND ADDRESS	10. PROGRAM ELEMENT, PROJECT, TASK AREA & WORK UNIT NUMBERS		
Air Force Geophysics Laboratory (LYU) Hanscom AFB Massachusetts 01731	62101F 8628 202 11 12		
11. CONTROLLING OFFICE NAME AND ADDRESS	12. REPORT DATE		
Air Force Geophysics Laboratory (LYU) Hanscom AFB Massachusetts 01731	3 Feb 1977		
14. MONITORING AGENCY NAME & ADDRESS (if different from Controlling Office)	13. NUMBER OF PAGES		
12 15 p.	17		
	15. SECURITY CLASS. (of this report)		
	Unclassified		
	15a. DECLASSIFICATION/DOWNGRADING SCHEDULE		
16. DISTRIBUTION STATEMENT (of this Report)			
Approved for public release; distribution unlimited.			
17. DISTRIBUTION STATEMENT (of the abstract entered in Block 20, if different from Report)			
9 Air Force surveys in Geophysics			
18. SUPPLEMENTARY NOTES			
19. KEY WORDS (Continue on reverse side if necessary and identify by block number)			
Weather satellites      Typhoons      Satellite imagery Infrared radiation      Hurricanes      Reentry system Visible radiation      Cloud ice      Typhoon reconnaissance Clouds      Cloud water Snow      Cloud mass			
20. ABSTRACT (Continue on reverse side if necessary and identify by block number)			
Several current programs in satellite meteorology at the Air Force Geophysics Laboratory are reviewed. First of all, the use of reflected sunlight at both visible and near infrared frequencies to distinguish snow from clouds is described. Secondly, a technique of compositing pictures of many typhoon cases in order to relate cloud features to typhoon motion is discussed. Finally, the use of visible and infrared imagery to estimate erosion parameters for reentry systems is described.			

DD FORM 1 JAN 73 1473 EDITION OF 1 NOV 65 IS OBSOLETE

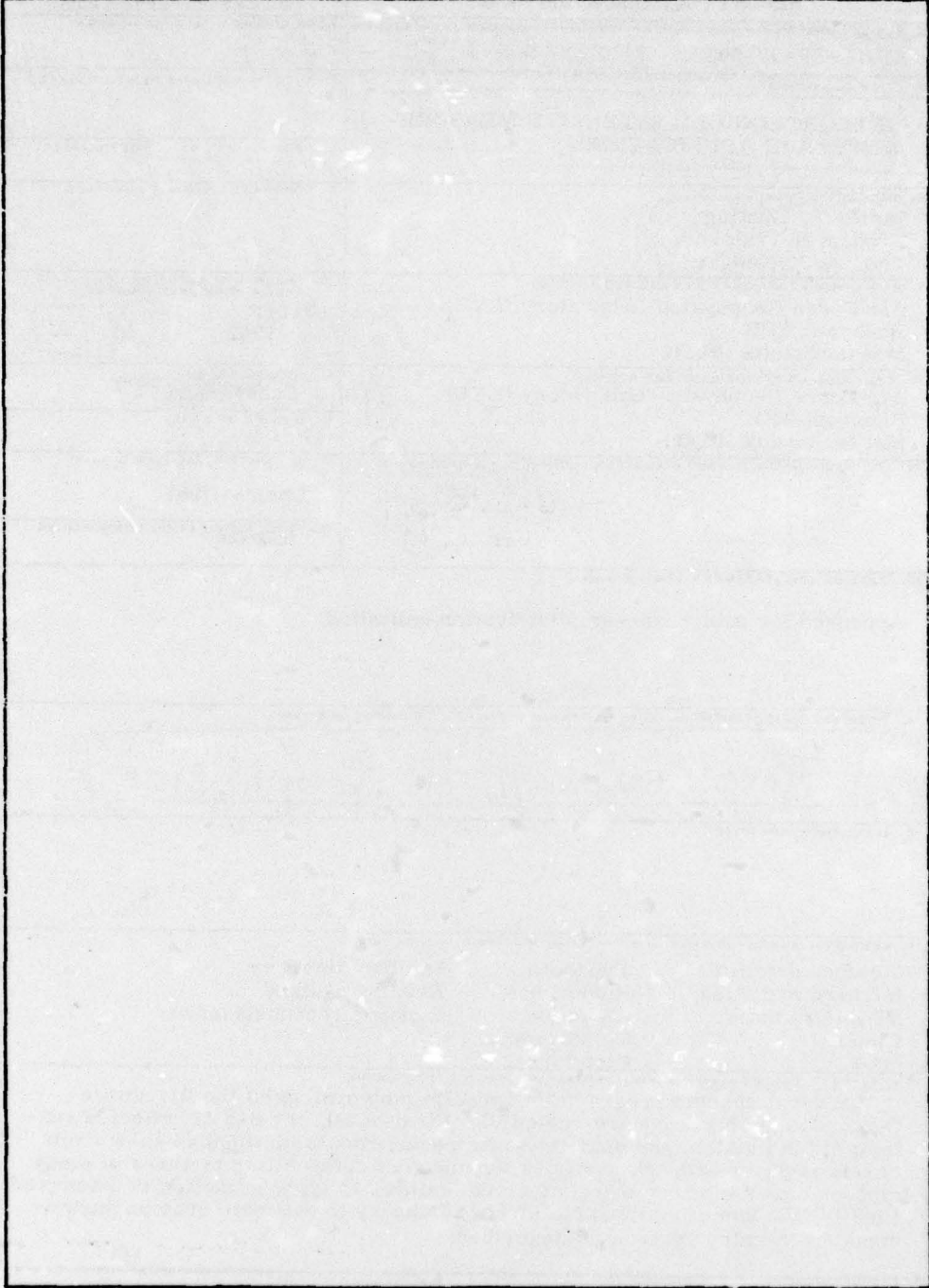
Unclassified

SECURITY CLASSIFICATION OF THIS PAGE (When Data Entered)

409 578

mt

SECURITY CLASSIFICATION OF THIS PAGE(When Data Entered)



SECURITY CLASSIFICATION OF THIS PAGE(When Data Entered)

## Preface

The Snow/Cloud Study has benefited from data, reports, and helpful discussions with many individuals from NASA and ERT, Inc. The Satellite Typhoon Study was conducted with extensive help from Mr. Robert F. Myers and the McIDAS team at AFGL. The Satellite Erosion Parameter Study would not have been possible without extensive data reduction by Mr. John Conover and many members of the Convective Cloud Physics Branch at AFGL.

ACC. SECTION for		
RTIS	White Section	<input checked="" type="checkbox"/>
BDC	Buff Section	<input type="checkbox"/>
UNANNOUNCED		<input type="checkbox"/>
JUSTIFICATION		
BY		
DISTRIBUTION/AVAILABILITY CODES		
D. L. SCALE 100% or SPECIAL		
A		

## Contents

1. INTRODUCTION	7
2. SNOW/CLOUD STUDY	8
3. SATELLITE TYPHOON STUDY	10
4. SATELLITE EROSION PARAMETER STUDY	13
REFERENCES	17

## Illustrations

1. Skylab Imagery of the Snow Covered Wasatch Range in Utah	9
2. Radiance Values Along Scan Lines From the Skylab S192 Multispectral Scanner	9
3. A Composite Picture of 4 Typhoons Moving Northwesterly	12
4. A Composite Picture of 5 Typhoons Moving Westerly	12
5. Aircraft Estimates of the Environmental Severity Index (ESI) of Clouds and Precipitation Compared to Simultaneous Satellite Measurements of Cloud Temperature From Infrared Sensors and Cloud Brightness From Visible Sensors	15
6. A Display of Visible Satellite Data Over the Central USA on 23 April 1975	16
7. A Display of Total Cloud Mass Estimates for 23 April 1975 Based on the Visible and Infrared Satellite Data	16

## Meteorological Satellite Measurements and Applications

### 1. INTRODUCTION

The Air Force Geophysics Laboratory (AFGL) supports the development of meteorological satellite systems by studies which help define future satellite instrumentation. Potential sensors have been studied for application to ultraviolet, near infrared, and microwave frequencies, to complement existing instrumentation at visible and infrared frequencies. AFGL also supports operating commands by studies which apply satellite measurements to detect and forecast troublesome clouds or atmospheric conditions. Better methods to sound for atmospheric temperature and moisture, as well as to detect cloud features have been sought.

In this report, 3 current studies have been chosen for review from the variety of potential topics: the use of  $1.6 \mu\text{m}$  imagery to distinguish snow from clouds, composite pictures of typhoons to predict typhoon motion, and the use of visible and infrared imagery to estimate erosion parameters for reentry systems. These studies are described in the following three sections.

---

(Received for publication 1 February 1977)

## 2. SNOW/CLOUD STUDY

The Air Force Air Weather Service has a requirement to provide automated analyses of clouds. Discrimination between snow and clouds from satellite imagery is often difficult so that cloud and/or snow analyses and forecasts are limited. A snow-cloud discriminator on board the Defense Meteorological Satellite Program (DMSP) satellite could remove these limitations and provide unique real-time data.

The Earth Resources Experiment Package (EREP) on Skylab provided an opportunity to examine the reflectance characteristics of snow and clouds from the visible to the near-infrared spectral region. The sensor used in this investigation is the S192 Multispectral Scanner which contains 13 bands covering the spectral range from 0.4 to 2.35  $\mu\text{m}$  and 10.2 to 12.5  $\mu\text{m}$ . Twelve of the bands are in the visible through the near-infrared portion of the spectrum (0.4 to 2.35  $\mu\text{m}$ ). The other band is located in the thermal infrared (10.2 to 12.5  $\mu\text{m}$ ). The S192 data output products are 70 mm screening film, digital data on Computer Compatible Tapes and line strengthened final film products.

Evaluation of Skylab EREP data for mapping snow cover has been conducted by Barnes et al.<sup>1</sup> The analysis of S192 imagery and digital tape data by the AFGL on the available Skylab data indicates a sharp drop in reflectance of snow in the near-infrared. Snow reflectance was essentially nonreflective in Band 11 (1.55 to 1.75  $\mu\text{m}$ ) and Band 12 (2.10 to 2.35  $\mu\text{m}$ ). An example of the marked drop in reflectance in the near infrared band can be seen in Figure 1. On the left of Figure 1, the high reflectance of snow in Band 2 (0.46 to 0.51  $\mu\text{m}$ ) over the snow-covered Wasatch Range in Utah can be seen from the S192 imagery. This same snow scene in the near infrared spectral range Band 11 (1.55 to 1.75  $\mu\text{m}$ ) on the right appears nonreflective (essentially black) in the S192 imagery.

Similar results were observed on other Skylab EREP passes. In addition, differences in the reflectance characteristics for snow, and between ice and water clouds in the visible and near infrared spectrum can be seen in the S192 imagery and from the digital data. A typical S192 radiance profile for Band 6 (0.68 to 0.76  $\mu\text{m}$ ) in the red part of the visible spectrum and Band 11 (1.55 to 1.75  $\mu\text{m}$ ) in the near-infrared portion of the spectrum is shown in Figure 2. The radiance values were obtained from processing the digital data from the S192 Computer Compatible Tapes. Band 6 (0.68 to 0.76  $\mu\text{m}$ ) is completely saturated for both snow cover (on the left) and clouds (on the right) in Figure 2. This saturation at a

1. Barnes, J.C., Smallwood, M.D., and Cogan, J.L. (1975) Study to Develop Improved Spacecraft Snow Survey Methods Using Skylab/EREP Data, ERT Document No. 0412F, Final Report, Contract No. NAS 9-13305, Environmental Research & Technology, Inc., Concord, Massachusetts.



Figure 1. Skylab Imagery of the Snow Covered Wasatch Range in Utah. Band 2 (0.46 to 0.51  $\mu\text{m}$ ) on the left shows the high reflectance of snow in the violet-blue spectral range. Band 11 (1.55 to 1.75  $\mu\text{m}$ ) on the right shows low reflectance of snow for this near infrared spectral range. EREP Pass 5, 5 June 1973 (from Barnes et al, 1975).

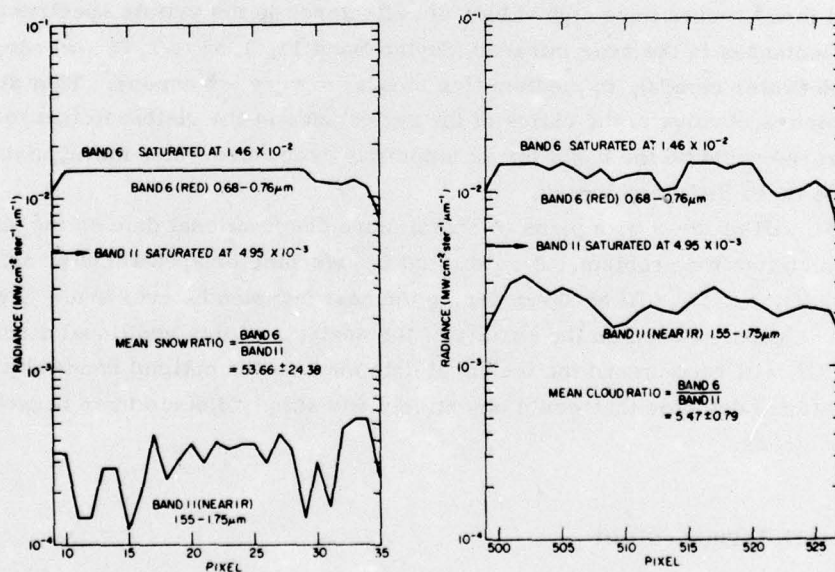


Figure 2. Radiance Values Along Scan Lines From the Skylab S192 Multispectral Scanner. The lefthand side has data taken over snow, while the right-hand side has data taken over water clouds

radiance value equal to  $1.46 \times 10^{-2} \text{ MW cm}^{-2} \text{ ster}^{-1} \mu\text{m}^{-1}$  in the digital data indicates a high reflectance in the visible part of the spectrum, and would appear white in the S192 imagery. In the near-infrared portion of the spectrum, Band 11 (1.55 to 1.75  $\mu\text{m}$ ) is saturated at a radiance value equal to  $4.95 \times 10^{-3} \text{ MW cm}^{-2} \text{ ster}^{-1} \mu\text{m}^{-1}$ . In the case of snow, shown on the left of Figure 2, the radiance values are much lower. The radiance values range from 1.25 to  $5.25 \times 10^{-4}$  and represent digital counts of 8 to 28 compared to 255 counts for saturation in Band 11. If 255 counts represents white, then counts of 8 to 28 would show black on S192 imagery. The mean snow ratio for Band 6/Band 11 is  $53.66 \pm 24.38$ . In the case of water clouds shown on the right of Figure 2, the radiance values range from 1.5 to  $3.25 \times 10^{-3}$  and represent counts of 78 to 168 in Band 11, which would show a relatively high reflectance or white on S192 imagery. The mean cloud ratio for Band 6/Band 11 is  $5.47 \pm 0.79$ . Cirrus or ice clouds seen on S192 imagery are highly reflective in Band 7 (0.78 to 0.88  $\mu\text{m}$ ) and exhibit a sharp decrease in reflectance in Band 11 (1.55 to 1.75  $\mu\text{m}$ ). This decrease in reflectance in Band 11 is seen as gray when compared with the "blackness" of snow in the near-infrared part of the spectrum.

The analysis of pairs of Skylab EREP S192 imagery, one set in the visible spectrum and one set in the near infrared, shows marked differences in the characteristic reflectances of snow, water clouds, and ice clouds in the two bands. While all three scenes have high values of reflectance in the visible spectrum, their reflectances in the near infrared (Skylab Band 11, 1.55 to 1.75  $\mu\text{m}$ ) range from high (water clouds), to medium (ice clouds) to very low (snow). This difference, which is obvious in the ratios of the reflectance in the visible to that in the near infrared could be the basis for an automatic procedure which distinguishes among the three different scenes.

AFGL will proceed with plans to obtain more observational data on the snow/cloud discrimination problem. A calibrated interferometer spectrometer aboard the AFGL/OP KC 135 will be flown during the next few months over snow, ice, and water clouds. Based on the results of the analysis of this additional aircraft data, AFGL will recommend the technical data such as the optimal bandwidth of the operational detector that would objectively and simply discriminate between snow and clouds.

### 3. SATELLITE TYPHOON STUDY

The satellite typhoon study supports the DoD Joint Typhoon Warning Center (JTWC) at Guam, which has responsibility for typhoon forecasts for the entire western Pacific and part of the Bay of Bengal. Satellite data are available to the

JTWC, and the AWS is under pressure to substitute satellite data for aircraft reconnaissance and to base forecasts on satellite observations wherever possible. The specific objective of the AFGL study is the prediction of 24-hour typhoon motion from satellite pictures alone.

Satellite pictures of clouds and clear areas represent physical processes going on in the atmosphere and are therefore a potential source of forecast information. The problem facing the satellite meteorologist who wishes to find the information, is how to manipulate and sort all the data present in complicated cloud fields in order to select those cloud features with predictive value. At AFGL, a technique has been applied that has been sorely needed but technically impractical since the first days of satellite meteorology; this is the technique of compositing. A composite is simply a field of average values derived from the superposition of a number of cases. The beauty of the compositing technique is that it will reinforce significant features of the cloud field and mute random details. The difficulty with compositing is the need to shift many typhoon pictures to some common frame of reference so that they can be averaged to form the composite picture. At AFGL, the necessary capabilities for satellite data processing are available on the Man Computer Interactive Data Access System (McIDAS) which was originally developed by the University of Wisconsin. Typhoons can be located on the CRT display, and then satellite imagery on the digital disk can be shifted to place typhoon centers at common coordinates and added by the McIDAS software.

Figures 3 and 4 are pictures of the McIDAS display with composite typhoon pictures. All the typhoons over a 3-year period that were located in a box from 15 to 20N latitude and 130 to 135E longitude at satellite pass time (about 00Z) were included. The typhoon cases were then divided into 2 categories of typhoon motion based on JTWC storm track data. Figure 3 is the composite of 4 typhoons moving northwesterly, while Figure 4 is the composite of 5 typhoons moving westerly. Visible pictures from NOAA satellites were averaged after the McIDAS shifted satellite data in order to superimpose storm centers. The storm centers are the brightest regions for each composite. The composite pictures outside the storm centers have some well-delineated cloudy and clear areas, and are not just neutral gray tones as would be expected if the clouds were randomly distributed about the typhoon. Moreover, significant differences in clear and cloudy areas outside the storm centers are evident in a comparison of Figures 3 and 4. In the case of northwesterly moving storms (Figure 3), the key feature is the well-defined clear area that extends from the west around to the north of the storms while outflow cloudiness is restricted to the eastern and southern quadrants of the storm. For the westerly moving storms (Figure 4), much more cloudiness exists to the northeast where it blends with midlatitude frontal cloudiness. This is the significant feature of westward moving storms in these latitudes and continues as the typhoons move westward into southeast Asia.

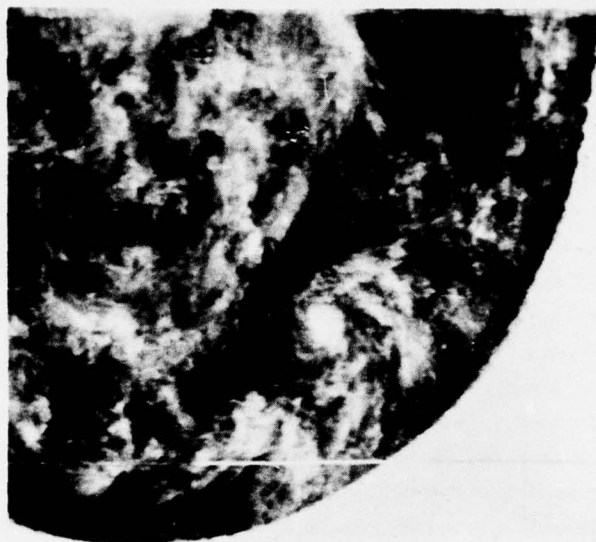


Figure 3. A Composite Picture of 4 Typhoons Moving Northwesterly. A well-defined clear area extends from the west around to the north of the storms

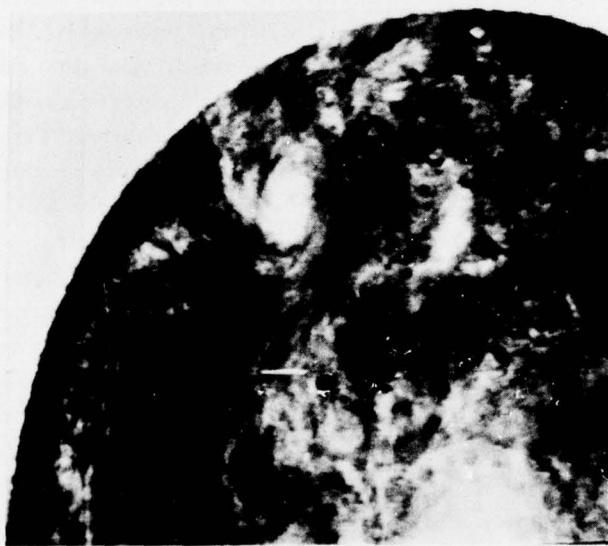


Figure 4. A Composite Picture of 5 Typhoons Moving Westerly. Compared to Figure 3, much more cloudiness exists northeast of the typhoon centers

Relationships between cloud distribution and typhoon motion are discussed in detail by Keegan<sup>2</sup> in a recent technical report, which gives similar results for investigation of typhoons in other areas. Program plans at AFGL will extend the work outlined in this preliminary report. Satellite data will be collected for more typhoon cases. Composite typhoon pictures will be made for infrared as well as visible satellite pictures. Also, geostationary satellite data will be collected for hurricane cases.

#### 4. SATELLITE EROSION PARAMETER STUDY

The USAF Advanced Ballistics Reentry Systems (ABRES) is the DoD lead agency for the design and development of new reentry systems. A significant design consideration for future systems is erosion of nose tips by cloud and precipitation particles. Engineering tests of various materials suggest that the mass density of hydrometeors is the most significant meteorological parameter related to weather erosion. AFGL supports weather erosion studies with an extensive program of cloud mass estimates by aircraft, radar, and satellites. In the satellite correlation study, satellite data have been directly compared to simultaneous cloud measurements by aircraft underflights. This method of direct comparison was chosen since it is difficult to model the radiative properties observed by satellites for ice particles with varying shape, size, and number concentration. A variety of cloud conditions has been sampled over the USA as well as the test ranges at Wallops Island and Kwajalein. Empirical relations have been derived to relate satellite infrared and visible measurements of clouds to weather erosion parameters.

A parameterization of clouds is necessary since reentry systems may encounter clouds at any altitude from the surface to the highest altitudes at which clouds are observed. The simplest erosion parameter is the vertical integral of cloud mass density over all cloud altitudes. ABRES has defined a more useful parameter as the Environmental Severity Index (ESI):

$$ESI = \int_{BASE}^{TOP} \rho h dh \quad (1)$$

2. Keegan, T.J. (1976) Cloud Distributions as Indicators of Tropical Storm Displacement, AFGL Technical Report 76-0170.

with  $\rho$  the cloud and precipitation mass density in  $\text{g/m}^3$ , and  $h$  the altitude in km. The ESI weights cloud mass by altitude since reentry vehicles move faster at higher altitudes and consequently suffer greater erosion.

A series of simultaneous measurements of clouds by satellites and aircraft has been conducted at AFGL. At the approximate time of the satellite pass, an aircraft equipped with cloud physics instrumentation would descend from 10 km altitude in a spiral of diameter 35 km at a descent rate of  $0.3 \text{ km min}^{-1}$ , to as low as air traffic control would permit. The aircraft measurements and supporting data such as rain gauge and radar records, were used to estimate cloud mass as a function of altitude. These estimates were then converted to erosion parameters such as total mass and ESI.

Aircraft estimates of ESI are related to satellite data in Figure 5. The correlation for total cloud mass was published earlier by Bunting.<sup>3</sup> In either case, the colder the cloud temperature as seen by the satellite infrared and the brighter the cloud as seen by the satellite visible, the higher the ESI or total cloud mass. These results were anticipated since satellite meteorologists have known for some time that cold and bright clouds indicate heavy weather. What we did not know before this series of measurements was the quantitative relationship between satellite data and cloud mass or ESI. The correlation coefficient ( $R$ ) comparing observations to estimates is 0.79 for ESI and 0.77 for total cloud mass. The reduction of variance ( $R^2$ ) is 0.62 for ESI and 0.59 for total cloud mass.

Figure 6 is a McIDAS display of visible satellite data over the central USA on 23 April 1975 taken from a NOAA archive. Bright dots for coastlines and state boundaries were added by a McIDAS subroutine. A cyclonic storm was developing with low pressure centered in northern Illinois and southern Wisconsin. Extensive cloudiness is evident over central USA and Canada. Most of the cloudiness is associated with the developing cyclone including convective activity in the warm sector (southern Illinois and Indiana) and an extensive cirrostratus shield over and north of the Great Lakes. Also evident are stratocumulus clouds in cold air over the Dakotas, and frozen Lake Winnipeg and James Bay. Figure 7, on the other hand, is a display of total cloud mass estimates based on visible and infrared satellite data in a relation similar to Figure 5. The highest estimates of cloud mass, from Illinois to southern Ohio, are in the southern half of the developing storm. The extensive shield of cirrostratus is detectable but has less cloud mass than the precipitating clouds to the south. The low stratocumulus in the Dakotas and frozen lakes, which are bright in the visible, are not evident in Figure 7 since they are

3. Bunting, J. T. (1976) Cloud properties from satellite infrared and visible measurements, Proceedings of the 7th Conf. on Aerospace and Aeronautical Meteorology and Symposium on Remote Sensing from Satellites, Melbourne, FL, 109-114.

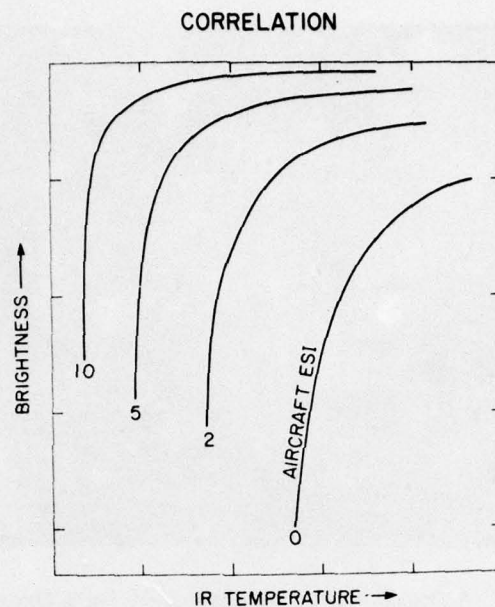


Figure 5. Aircraft Estimates of the Environmental Severity Index (ESI) of Clouds and Precipitation Compared to Simultaneous Satellite Measurements of Cloud Temperature From Infrared Sensors and Cloud Brightness From Visible Sensors. The curves for ESI equal to 0, 2, 5, and 10 are solutions to a regression equation relating aircraft ESI measurements to satellite data

warmer than the clouds associated with the cyclone. Figure 7 also compared well with the National Radar Summary since the areas of high cloud mass are also areas of precipitation.

A more complete description of this work appears in reports by Bunting and Conover.<sup>4, 5</sup> Program plans at AFGL will apply the satellite correlations to one year of satellite data to generate a climatology of potential weather erosion to be used in the design of future reentry systems.

4. Bunting, J. T., and Conover, J. H. (1976) The Use of Satellite Data to Map Excessive Cloud Mass. AFCRL Technical Report 76-0004.
5. Bunting, J. T., and Conover, J. H. (1976) Estimates from satellites of total ice and water content of clouds, Proceedings of the International Conf on Cloud Physics, Boulder, CO, 407-412.

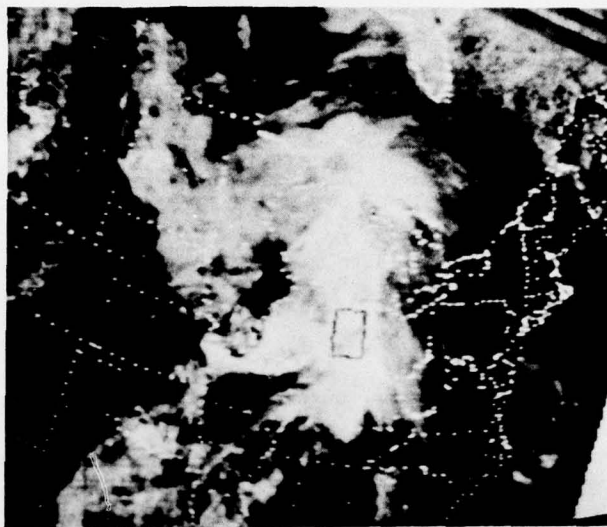


Figure 6. A Display of Visible Satellite Data Over the Central USA on 23 April 1975. An aircraft sampled clouds over western Indiana, in an area indicated by a dark box

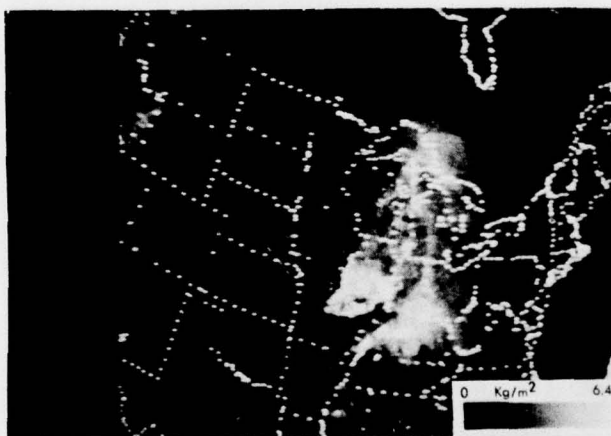


Figure 7. A Display of Total Cloud Mass Estimates for 23 April 1975 Based on the Visible and Infrared Satellite Data. A gray scale relating image brightness to cloud mass is in the lower right

## References

1. Barnes, J.C., Smallwood, M.D., and Cogan, J.L. (1975) Study to Develop Improved Spacecraft Snow Survey Methods Using Skylab/EREP Data, ERT Document No. 0412F, Final Report, Contract No. NAS 9-13305, Environmental Research & Technology, Inc., Concord, Massachusetts.
2. Keegan, T.J. (1976) Cloud Distributions as Indicators of Tropical Storm Displacement, AFGL Technical Report 76-0170.
3. Bunting, J.T. (1976) Cloud properties from satellite infrared and visible measurements, Proceedings of the 7th Conf. on Aerospace and Aeronautical Meteorology and Symposium on Remote Sensing from Satellites, Melbourne, FL, 109-114.
4. Bunting, J.T., and Conover, J.H. (1976) The Use of Satellite Data to Map Excessive Cloud Mass. AFCRL Technical Report 76-0004.
5. Bunting, J.T., and Conover, J.H. (1976) Estimates from satellites of total ice and water content of clouds, Proceedings of the International Conf on Cloud Physics, Boulder, CO, 407-412.